

# A Silicon Photonic Interferometric Router Device Based on SCISSOR Concept

Marco Masi, Mattia Mancinelli, Alberto Battarelli, Romain Guider, Manga Rao Vanacharla, Paolo Bettotti, Jean-Marc Fedeli, and Lorenzo Pavesi, *Senior Member, IEEE*

**Abstract**—A novel wavelength routing device for optical on-chip network applications is presented. It is based on the constructive and destructive interferences that occur when two side-coupled integrated spaced sequences of resonators (SCISSORs) are coupled in parallel to a single common waveguide. Its potential application for coarse wavelength division multiplexing, i.e., band routing functionalities, and its robustness against fabrication tolerances and signal imbalances are analyzed. Design, simulation, fabrication, and experimental characterizations are described. We compare measurements of the fabricated device with simulations for the ideal and the actual device, where random variations in the geometrical parameters inherent in the fabrication process are considered. This allows demonstrating the concept of interferometric SCISSOR routing and to discuss the limits and advantages of coupled resonator-based design for routing.

**Index Terms**—Filtering, microresonators, photonic switching systems.

## I. INTRODUCTION

IF the increase of the number of processing cores would follow the same pace of Moore's law, an increasingly large-bandwidth and low-power communication infrastructure becomes an unavoidable option. Optical networks on chip (ONC) envisage core-to-core photonic interconnects with large bandwidth, ultrafast switching, ultralow power consumption, and support of optical wavelength division multiplexing (WDM) methods [1], [2]. In particular, silicon photonics has shown to be a viable interconnect technology [3]–[5], [34]. Silicon-on-insulator (SOI) photonic structures

offer compatible fabrication processes with CMOS technology. Microdisk lasers, photodetectors, ring filters, and flip-flop memory cells were demonstrated with promising performances and a potential for ONC and all-optical signal processing [6]–[8]. In this context, while the theory and implementation of single microring resonators were extensively investigated (e.g., [9]–[12], and references therein), practical realizations of cascaded resonators (e.g., side-coupled integrated spaced sequences of resonators (SCISSORs) and coupled resonator optical waveguide [13]–[18]) were studied to a smaller extent [19]–[22]. In this paper, we report about the design, fabrication, and characterization of a wavelength router device based on the coupling of two SCISSORs and on the interplay between the phase of the optical signals. This photonic device is fabricated with silicon photonics technology. Its potential could span from coarse WDM (CWDM) to pipeline forwarding techniques (optical node-to-node packet forwarding during predefined time frames [23]).

## II. CONCEPT LAYOUT

SCISSORs are based on a sequence of either ring or racetrack resonators that are coupled by two side waveguides. For this reason, SCISSORs are characterized by two different kinds of resonances: the first due to the isolated resonators and the second due to the coherent Bragg scattering of light from the resonator sequence [21]. Both type of resonances contribute to the SCISSOR spectrum. The particular SCISSOR geometry we are going to consider is based on a sequence of racetrack resonators instead of the more often used ring resonators. Racetracks have a longer coupling section than rings which makes more effective the coupling of light in TE-polarization. In fact, TE modes are more confined in the waveguide than TM modes. The long coupling section allows an easier tuning of the coupling by simply varying the straight part of the racetrack instead of controlling the waveguide-ring gap spacing. Moreover, the simulation of racetrack-based SCISSOR turns out to be easier than for ring-based SCISSOR since coupled mode theory of the coupling constants between two straight waveguides is relatively simpler than between a ring and a straight waveguide where more complicated physical and analytical considerations are involved [26].

In this paper, we propose to use the coherent overlap of light resonant with two identical SCISSOR for interferometric routing and switching. The proposed structure is depicted in Fig. 1. It is composed of two input waveguides  $In_1$  and  $In_2$  that are coupled to two SCISSOR devices. The two SCISSORs are in turn coupled by a common central waveguide that identifies the drop output port of the router. Depending on the wavelengths of the input signals and their relative phase difference,

Manuscript received January 05, 2011; revised May 11, 2011; accepted June 06, 2011. Date of publication June 16, 2011; date of current version August 26, 2011. This work was supported by the EU under the FP7 ICT-(216405) Project Wavelength Division Multiplexed Photonic Layer on CMOS.

M. Masi was with the Nanoscience Laboratory, Department of Physics, University of Trento, 38122 Trento, Italy. He is now with the Institut des Nanotechnologies de Lyon, Institut National des Sciences Appliquées de Lyon, 69621 Villeurbanne, France (e-mail: masi@science.unitn.it).

M. Mancinelli, M. R. Vanacharla, P. Bettotti, and L. Pavesi are with the Nanoscience Laboratory, Department of Physics, University of Trento, 38122 Trento, Italy (e-mail: mancinielli@science.unitn.it; manga@science.unitn.it; bettotti@science.unitn.it; pavesi@science.unitn.it).

A. Battarelli was with the Nanoscience Laboratory, Department of Physics, University of Trento, 38122 Trento, Italy. He is now with Trentino Network, 38121 Trento, Italy (e-mail: a.battarelli@studenti.unitn.it).

R. Guider was with the Nanoscience Laboratory, Department of Physics, University of Trento, 38122 Trento, Italy. He is now with the Institut für Halbleiter und Festkörperphysik, Linz University, A-4040 Linz, Austria (e-mail: guider@science.unitn.it).

J.-M. Fedeli is with the Electronics and Information Technology Laboratory, French Atomic Energy Commission, 38054 Grenoble Cedex 9, France (e-mail: jean-marc.fedeli@cea.fr).

Color versions of one or more of the figures in this paper are available online at <http://ieeexplore.ieee.org>.

Digital Object Identifier 10.1109/JLT.2011.2159826

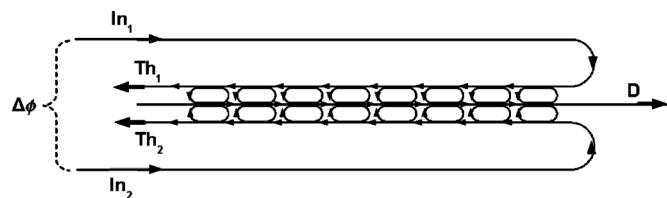


Fig. 1. SCISSOR router formed by two coupled eight racetrack SCISSOR. Two input signals ( $In_1$  and  $In_2$ ) are inserted in the router from the left. If they have a wavelength resonant with the racetrack resonances and a phase difference  $\Delta\phi = \pi$ , then light interferes destructively at the central common waveguide and the signal  $D$  on the drop port is zero, whereas the signals are transmitted to the through ports. If instead a phase difference  $\Delta\phi = 0$  is applied at the inputs, then light interferes constructively at the central common waveguide and the signal exits on the drop port, consequently the signals ( $Th_1$  and  $Th_2$  in the through ports vanish).

two ideally equal intensity input signals ( $In_1 = In_2$ ) are either transmitted to the through output ports  $Th_1$  and  $Th_2$  or to the drop port  $D$ . When the two input signals are out of phase ( $\Delta\phi = \pi$ ), as shown in Fig. 1, they interfere destructively in the common waveguide, no signal is transmitted to the drop port, and the signals are transmitted to the through output ports. If their phase relation is such that constructive interference occurs in the central waveguide ( $\Delta\phi = 0$ , Fig. 1), the two signals add coherently and a signal is transmitted to the drop output port. Due to power conservation, in an ideal lossless system, this constructive interference produces a signal whose intensity is given by the sum of the two input intensities.

In Fig. 1, two parallel eight racetrack SCISSORs are shown. It is clear that the same interferometric routing can be achieved by using a lower number of resonators, e.g., a single resonator pair. However, there are several reasons why SCISSOR is advantageous over single resonator geometries. For example, let us consider a situation where strong imbalances between the inputs are present. Fig. 2 illustrates a transfer matrix simulation of the balanced and imbalanced cases (solid and dashed lines, respectively). Propagation and bending losses of 3 dB/cm and 0.025 dB/90°, respectively, are considered in the simulation [27]. In the balanced case ( $In_1 = In_2 = 1$ ), it is observed that the drop signal is almost 2 for  $\Delta\phi = 0$ , while it decreases to zero increasing  $\Delta\phi$  to  $\pi$ . Concurrently, the through signals are zero for  $\Delta\phi = 0$  and increase to almost 1 for  $\Delta\phi \rightarrow \pi$ . Note that both  $D \neq 2$  or  $Th_1 \neq 1$  and  $Th_2 \neq 1$  due to the finite propagation losses are assumed. The slight asymmetry between the  $Th_1$  and  $Th_2$  signals is caused by the small differences in their resonant band gap [e.g., see later in Fig. 8(left)]. If  $In_1$  and  $In_2$  are different in intensities while resonant with the SCISSOR, the  $D$  signal decreases significantly for  $\Delta\phi = 0$ : the effect of the input imbalance starts to be sizeable for a 50% imbalance. Fig. 2 shows the  $D$ ,  $Th_1$ , and  $Th_2$  signals for an imbalance of 75% ( $In_1 = 1; In_2 = 0.25$ ). It is noted that the  $D$  signal does not vanish when  $In_1$  and  $In_2$  signals are out of balance, while the two  $Th_1$  and  $Th_2$  signals are still equal. This is because in an eight pair SCISSOR router, the signals that resonate with the first pair of resonators provide less imbalanced inputs into the following pair, and so on. At the end of the resonator chain, the balance between the two signals is restored and their intensities sum up to the sum of the two inputs. Fig. 3 shows how the imbalance affects the maximum of the  $Th_1$  or  $Th_2$  signals (at  $\Delta\phi = 0$ )

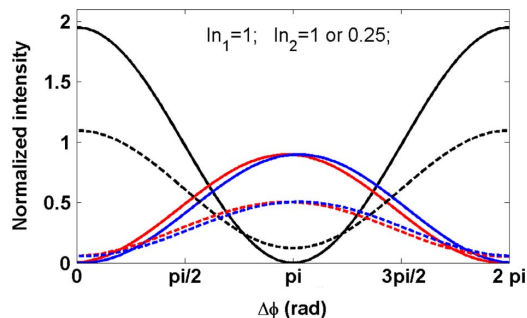


Fig. 2. SCISSOR router phase response with no inputs imbalance (solid lines) and 75% inputs imbalance (dashed lines). The input signal intensities are labeled  $In_1$  and  $In_2$ , the output signals are the two through signals  $Th_1$  (red line),  $Th_2$  (blue line), and the drop signal  $D$  (black line).

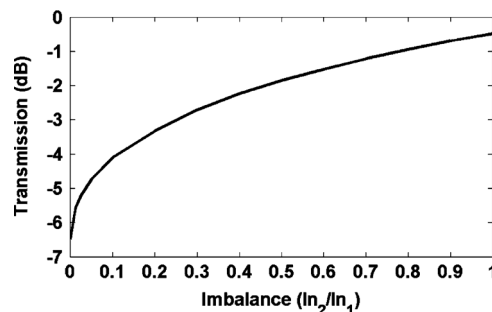


Fig. 3. Through port intensity (at  $\Delta\phi = 0$ ) of the SCISSOR router as a function of the input imbalance. Only the intensity of one through signal is reported since the SCISSOR router response is symmetric with respect to the through exit ports.

by varying the imbalance of the inputs. This is particularly interesting because it demonstrates that this kind of router recovers possible intensity difference in its inputs. Such an effect is not achievable by using a router formed by only two resonators.

Another reason to use many side-coupled resonators instead of few is to achieve a better coupling of the input signals with the central waveguide for  $\Delta\phi = 0$ . This leads to a sharper difference in the drop signal as a function of the phase. Moreover, as we will demonstrate in the next sections, lithographic fabrication imperfections tend to be averaged out with a high number of resonators which yields a more robust design. Finally, the full-width at half-maximum of the SCISSOR resonances is larger for an increased number of resonators that is needed for band routing functionalities. When the resonator spacing ( $d_R$  is the distance between two nearby resonators) is chosen so that the resonator modes and the Bragg modes overlap ( $d_R = \pi R$ , where  $R$  is the radius of the curved part of the racetrack), then also a larger free spectral range is obtained ([13]–[18], [24]). These facts are shown in Fig. 4(a) where 1, 2, 4, and 8 resonator SCISSORs are compared (the geometrical parameters of the structure will be given in Section III).

Practically, the resolution in the lithography used to produce the router causes fabrication errors. These affect all SCISSOR devices [21] since they cause random statistical variations of the SCISSOR parameters (racetrack geometrical parameters, racetrack to waveguide gap, relative positions of racetracks with respect to the common waveguide, etc.) at the nanometer scale. These variations affect also the relative phase of the signals since their optical paths might differ. A comparison of the drop

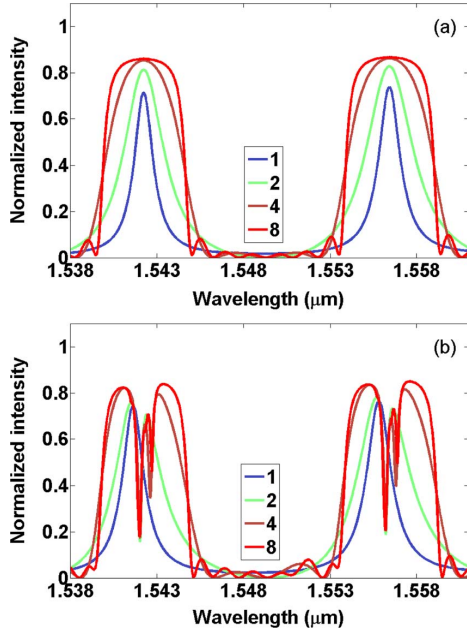


Fig. 4. Spectral response of a single SCISSOR formed by a different number of racetrack resonators: blue line for one single resonator, green line for two resonators, magenta line for four resonators, and red line for eight resonators. (a) Ideal spectrum. (b) Example of spectral impairment caused by random fabrication imperfections.

signal spectrum of an ideal SCISSOR [see Fig. 4(a)] and of a SCISSOR with 5 nm random variation in the geometrical parameters [see Fig. 4(b)] shows the appearance of noisy dips within the resonance band. These dips are evidence of disorder-induced optical mode localization as discussed in [21]. Their presence limits the range of wavelengths that can be properly routed by SCISSOR.

### III. MODELING, MASK DESIGN, AND FABRICATION

The modeling and simulation of the router were performed via three steps: waveguide parameter estimation, circuit response modeling, and silicon device component simulation. Parameter estimation was carried out with a full-vectorial finite-difference mode solver [28]. For instance, we had to determine the wavelength-dependent racetrack coupling section lengths and the coupling constants. From these parameters, we obtain the proper gap spacings. Results are published in [24]. With these parameters, we perform the simulations of the spectral response of the single SCISSOR and their combination as in the proposed geometry to analyze the drop and through port signals as a function of the phase difference of the input signals. This was done by using a transfer matrix method applied to each block of the coupled SCISSOR structure [25]. Finally, we simulate the other photonic components in the router like waveguide crossings, multimode interference (MMI) splitters, and tapers. These were designed with a commercial finite-difference time domain package. All simulations assumed TE-polarization and SOI waveguides.

Fig. 5 reports the layout of the router. The input ports have been separated by a distance that allows the simultaneous use of two tapered fibers to input the signals. Reference waveguides are used to monitor the input signals that reach the SCISSOR. To this end, an MMI splits the input signal in two waveguides: the

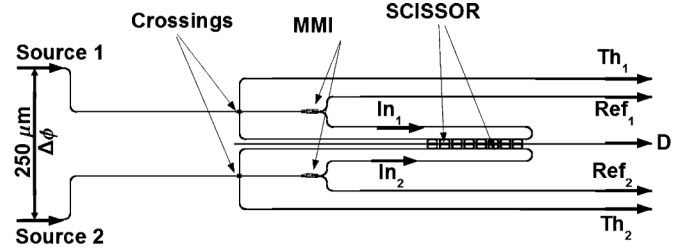


Fig. 5. Layout of the SCISSOR interferometric switch in Fig. 1. Codirectionality between input and output is achieved by bending the Th<sub>1</sub> and Th<sub>2</sub> signals on the right device side.

reference waveguide and the real SCISSOR input waveguide (it is the signal in these waveguides that we have used in the previous calculation and called In<sub>1</sub> and In<sub>2</sub>). It is also desirable to have all the inputs on one side and the outputs on the other side. For this reason, the waveguide after the SCISSOR is bent to take the through signals on the right device side. This forced us to insert two waveguide crosses.

This design was then transferred to a mask and processed on SOI wafers by using the processing facilities of CEA-LETI. The wafers were 200 mm SOI wafers with a 220 nm thick silicon and 2 μm thick buried oxide. The pattern definition was achieved by using state of the art deep ultraviolet 193 nm lithography. Different exposure doses were used to change few critical feature sizes, such as the gaps. The silicon waveguide and the other photonic components were then covered by a 0.75 μm thick SiO<sub>2</sub> layer that acts as a waveguide cladding layer as well as a protective layer. The waveguides were designed with a width of 0.5 μm; the waveguide-racetrack gaps were 200 nm; the racetracks have a radius of  $R = 3.25 \mu\text{m}$  and a straight section of  $L = 10 \mu\text{m}$ . For this radius, the process yields a measured bending losses of about 0.025 dB/90° (measurements done on a series of 100 bends) [27]. It is customary to define the distance  $d_R$  as the distance between the centers of the half circumference of two facing racetracks. In our case  $d_R = 10.21 \mu\text{m}$ . To decrease the coupling losses, tapering of each input and output waveguides was used. A 500 μm long adiabatic taper reduced the waveguide width from 2 μm down to 0.5 μm. The crossings and MMI splitters were processed by using a double etch processes in which a 70 nm shallow etch is followed by a 150 nm deep etch. This double etch scheme was based on the low insertion losses cross design of [29]. Measurements on a chain of cascaded crosses show 0.35 dB loss per crossing with a crosstalk of about -27 dB and a back reflection of 0.17% while the major contribution to losses (3.6%) comes from scattering. The MMI design was the same as in [7] and had about 0.4 dB insertion losses with, however, a strong impairment between the two output channels possibly due to layer misalignment during the fabrication process. This impairment made very difficult the use of the reference signals for intensity normalization.

### IV. EXPERIMENTAL CHARACTERIZATION AND RESULTS

The setup used to test the router is shown in Fig. 6. It is a standard setup for waveguide measurements apart the input section. In fact, we need two input signals that are coherently controlled in phase. To achieve this, the output of a single continuous-wave tunable laser is connected via a fiber splitter to two

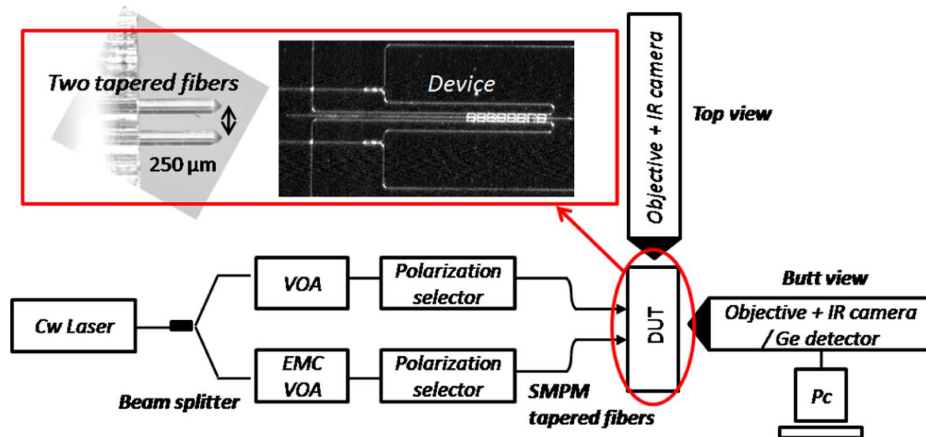


Fig. 6. Experimental setup used to test the router (VOA: variable optical attenuator, EMC: electromechanical, SMPM: single mode polarization maintaining, and DUT: device under test).

polarization maintaining fibers. Each fiber is then connected to a polarization selector and a variable optical attenuator (VOA) in order to independently tune the polarization and intensity of the signal in each fiber. One of the VOA (named electromechanical (EMC)-VOA) can be controlled electromechanically in order to have an attenuation sweep linear in time. Due to the fact that attenuation in the VOA is achieved by moving apart the input and output VOA fibers, an attenuation change leads also to a different optical path in the VOA which, in turn, translates into a phase change of the optical signal. Note that the phase is much more sensitive to the distance than the intensity so the phase changes more rapidly than the intensity. Therefore, during the attenuation sweep, we achieve a phase shift of the signal in a fiber with respect to the one in the other which causes the oscillatory behavior of the signals in Fig. 9. The two fibers are then connected to two polarization maintaining tapered fibers that are mounted on a special holder with two V-groove separated by  $250\ \mu\text{m}$ . The signals are then coupled into the device under test (DUT) by butt coupling where the fiber to waveguide alignment is controlled by a nanometer piezoelectric positioning system. This experimental setup allows to get the DUT response either to a wavelength scan of one of the two input signals or to a relative phase scan of the two input signals with a fixed wavelength.

The five output signals ( $\text{Ref}_1$ ,  $\text{Ref}_2$ ,  $\text{Th}_1$ ,  $\text{Th}_2$ , and D) are then measured either independently and in sequence with an optical zoom coupled to a Ge detector or simultaneously by imaging the whole output facet of the DUT into an IR charged-coupled device camera. Then, by an image processing software, the intensity of each spots corresponding to each output is obtained as a function of the input signals. The setup allows also imaging the scattered light on the DUT surface into another IR camera and by image processing select specific router area to measure the intensity of the scattered light as a function of the input signals.

The first measurement performed is the spectral response of the router. We scan a resonator resonance and not a Bragg resonance. In fact for a Bragg resonance neither the drop nor the through signals go to zero in resonance [21]. Our experimental setup does not allow to perform a wavelength scan for a controlled and fixed phase difference between the two inputs. For this reason, we could only make a wavelength scan for a single

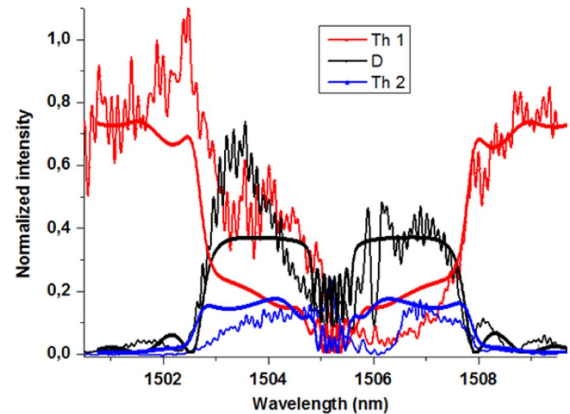


Fig. 7. Through and drop port spectra (black, blue, and red lines, respectively) measured for the eight racetrack SCISSOR router when a single signal  $\text{In}_1$  is input. The intensity at the through port 2 ( $\text{Th}_2$ , blue line) gives the crosstalk. The thick continuous line represents the theoretical expected response.

input. For a single input, the drop and two through spectra are reported in Fig. 7. We observe a wide passband that extends for almost 6 nm. Here, the signal instead of being transmitted to the through ports is resonantly coupled with the central waveguide (drop signal, black line). Due to the limit in the processing, few dips appear in the center of the passband. The dips in the passbands limit the available spectral range to the two lateral sidebands. Because of the power splitting imbalance in the MMI, the measured spectrum is asymmetric with respect to the resonance as would be expected in the ideal structure. Despite these experimental limitations, the agreement between the measured and simulated spectra is satisfactory. It is interesting to note the large crosstalk from channel 1 to channel 2 as measured by the signal at the output through port 2 (blue line). When the signal wavelength is within the passband, the signal leaks to the other output through port.

The simulated spectrum with a signal only in the  $\text{In}_1$  (the continuous lines in Fig. 7) is shown also in Fig. 8(left) to compare it with the case where both inputs are injected with an equal intensity and are in phase (see Fig. 8(right), the red and blue curves overlap). In this way, we can evaluate the crosstalk and the response under strongly imbalanced inputs. We note that for the former case [see Fig. 8(left)], the drop signal shows an intensity

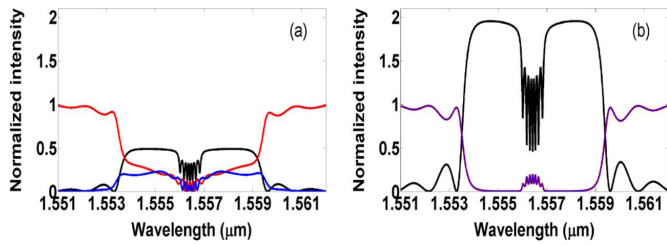


Fig. 8. Spectra of the  $Th_1$  (red line),  $Th_2$  (blue line), and D (black line) outputs for the eight racetrack SCISSOR router with only one input signal (left) and both input signals with the same phase (right).

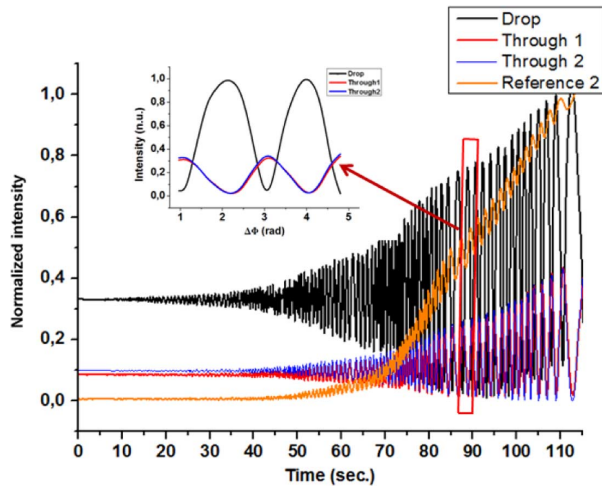


Fig. 9. Drop (black line), through 1 (red line), through 2 (blue line), and  $Ref_2$  (orange line) signals as a function of the amplitude sweep of one of the two input ( $In_2$ ) of the eight SCISSOR router in Fig. 5. (Inset) Phase response of the device when the two input signals have the same intensity (red box region in the main graph).

that is only half the one of the input. The  $Th_1$  signal is complementary to the D signal with two remarkable features: out of the passband its intensity reaches almost 1 and in the passband it does not go to zero. This is due to the crosstalk between the two SCISSORs which causes a nonzero signal intensity also at the  $Th_2$  output in the wavelength range of the passband. To decrease the crosstalk, one has to balance the intensity of the input signals and increase the number of resonators in the SCISSOR. This is shown in Fig. 8(right), where the simulations are performed for the same structure but with two input signals of same intensity and phase. Now the spectral response is the one expected with two equal output through signals and zero through signal in the passband.

The phase dependence of the outputs from the router when the signal wavelength is within the drop passband is shown in Fig. 9. A signal wavelength of 1534.95 nm was used. The phase change was obtained by sweeping in time the attenuation of the EMC-VOA ( $In_2$  intensity sweep). We then correlate the time with the phase shift by using the  $2\pi$  periodicity of the oscillations of the output signals. The response of the router when the two input signals have equal intensity can be found when the D signal vanishes (red box in the figure, blow up in the insert).

The black, red, and blue lines represent the D,  $Th_1$ , and  $Th_2$  signals, respectively. The orange line represents the  $Ref_2$  signal (reference for  $In_2$ ). It is observed that the phase difference between the inputs affects significantly the drop signal only when

the two input channels are increasingly balanced. In fact, the oscillations on the D signal are large only when  $Ref_2$  increases. In addition, the same behavior in the  $Th_1$  and  $Th_2$  signals is observed. A detail of the phase response of the router when the inputs are balanced is shown in the inset of Fig. 9. Clear oscillations due to constructive and destructive interference on the central waveguide are observed both in the drop and through signals. This proves that the routing is controlled both by the phase and by the wavelength, i.e., the device is an interferometric wavelength router. Where the input signal is routed depends both on the signal wavelength and on the signal phase. The observed profiles are not perfectly sinusoidal for an experimental limitation that is related to the noisy mechanical sweep of the EMC-VOA. Due to losses, mainly scattering losses, the sum of the two out-of-phase through signals does not equal the in-phase drop signal. This is also observed in the simulations in Fig. 2. Note also how, in the balanced case, the two through signals are almost equal, as expected from the simulations. This correspondence is not always observed due to the slight asymmetries of the through response.

Fig. 10 shows the comparison between the phase response for two routers: one based on one racetrack pair (see Fig. 10(a),  $\lambda = 1542.25$  nm), and the second based on eight racetrack pairs (see Fig. 10(b),  $\lambda = 1534.95$  nm). In addition, we show in Fig. 10(c) the top scattering curves of the eight racetrack pair router ( $\lambda = 1528.6$  nm). These are taken by numerically integrating a given portion of the top IR image of the DUT: the area of the central common waveguide for the black curve (the resulting intensity is proportional to the drop signal) and that of the eight pairs of racetracks for the orange curve (the resulting intensity is proportional to the light intensity propagating in the resonators). From these data, it emerges that both one and eight pair routers follow the predicted behavior. In particular, the one pair design shows an extinction in the drop channel of 9 dB and the amplitudes of the through signals in destructive interference state sum up to the value of the drop signal in constructive interference state. This means that this design has a good capacity of redirecting the signals in the through ports without introducing significant losses. It is, however, observed a shift between the extreme of the drop and the two through signal maxima. This is probably due to a nonperfect alignment of the center of the racetracks which introduces a further uncontrolled phase shift for the signal propagating in one or the other through waveguides. On the other hand, the eight pair design shows a drop extinction of 15 dB, thanks to the higher number of racetracks. However, extra losses are observed and the through signals have lower intensities than for the one pair resonator router. Fig. 10(c) shows the origin of these extra losses. When the drop signal shows a minimum in the scattered intensity, the interference is destructive. In this case, we observe that the scattered intensity in the SCISSOR is maximum. These observations show that, when destructive interference occurs in the common waveguide, the light signal couples back into the racetracks where it is partially radiated by the scattering. This behavior is detrimental for routing and needs to be improved for practical purposes.

Another effect that can be noted in Fig. 10(b) and (c) is the phase offset between the drop and the two through signals. This is a consequence of the random variations in the racetrack parameters, which randomize in turn the relative phase of the drop and the two through signals. If the input signals  $In_1$  and  $In_2$  are

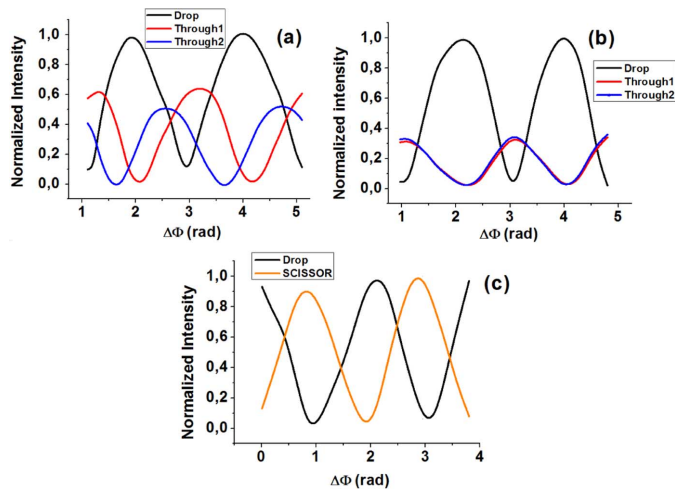


Fig. 10. (a) Phase response of a one pair SCISSOR router ( $\lambda = 1542.25$  nm) and (b) of an eight SCISSOR router ( $\lambda = 1534.95$  nm). (c) Top scattering of the eight SCISSOR router from the common waveguide area (D channel, black line) and from the resonators area (orange line) ( $\lambda = 1528.6$  nm). All graphs are normalized to the maximum amplitude of the D channel.

TABLE I  
COMPARISON OF THE PHASE ( $\Delta\Phi_{1,8}$ ) AND AMPLITUDE ( $\Delta A_{1,8}$ ) DIFFERENCES BETWEEN THE ONE PAIR (LEFT) AND EIGHT SCISSOR (RIGHT) ROUTERS

$\Delta\Phi_1 \pm \sigma_{\Phi_1}$	$\Delta A_1 \pm \sigma_{A_1}$	$\Delta\Phi_8 \pm \sigma_{\Phi_8}$	$\Delta A_8 \pm \sigma_{A_8}$
$0.34 \pm 0.12$	$0.4 \pm 0.17$	$0.02 \pm 0.03$	$0.24 \pm 0.15$

in phase, they have, nevertheless, to go through two different optical paths if the resonators differ. This leads to an offset of the drop signal from the ideal expected extinction at phase difference  $\Delta\Phi = 0$ . To quantify this, we measured seven different but nominally equal one and eight SCISSOR routers. We statistically quantify the influences of fabrication variations by measuring the phase difference between the two through signals ( $\Delta\Phi_1$  and  $\Delta\Phi_8$  for the one and eight SCISSOR router, respectively), and their maximum amplitude difference

$$\Delta A = \frac{|Th_1 - Th_2|}{(Th_1 + Th_2)/2}.$$

Table I reports the average values for the one and eight SCISSOR router (left and right, respectively). It is observed that the eight SCISSOR router is much more robust with respect to fabrication variations (smaller averages) than the one pair router. This is a consequence of the collective behavior of the SCISSOR which smoothes out statistical imperfections with an increasing number of resonators. Therefore, there is a tradeoff between the robustness and the losses when designing the number of racetracks in the SCISSOR router.

## V. CONCLUSION

We designed, fabricated, and characterized a novel photonic interferometric wavelength routing device based on SCISSOR. We show that the interferometric wavelength router has band routing functionalities and is robust against fabrication imperfections and input signal imbalances. These are clear advantages over more conventional Mach-Zehnder or single resonator

routers. The experimental test furnished a first demonstration of the viability of the concept: signal routing and switching are controlled by the phase difference of two input signals as well as by their wavelength. Current fabrication technologies limit the usefulness of this router because of random variations of its geometrical parameters induced by processing limitations. Nevertheless, it is shown that the proposed device works as expected and that its behavior is well understood. We believe that further design optimizations and especially the upcoming of new lithographic technologies will dramatically improve the device performances. Next generation electron beam- or extreme ultraviolet lithography promise to lower fabrication errors by an order of magnitude, making the proposed SCISSOR-routing and interferometric-switching systems a valuable approach that can complement other existing routing and switching technologies.

## REFERENCES

- [1] D. A. B. Miller, "Device requirements for optical interconnects to silicon chips," *Proc. IEEE*, vol. 97, no. 7, pp. 1166–1185, Jul. 2009.
- [2] A. Shacham, K. Bergman, and L. P. Carloni, "Photonic networks-on-chip for future generations of chip multiprocessors," *IEEE Trans. Comput.*, vol. 57, no. 9, pp. 1246–1260, Sep. 2008.
- [3] L. Pavesi and D. Lockwood, "Silicon photonics," in *Topics in Applied Physics*. New York: Springer-Verlag, 2004, vol. 9.
- [4] S. J. B. Yoo, "Future prospects of silicon photonics in next generation communication and computing systems," *Electron. Lett.*, vol. 45, no. 12, pp. 584–588, Jun. 2009.
- [5] A. Joshi, C. Batten, Y.-J. Kwon, S. Beamer, I. Shamim, K. Asanovic, and V. Stojanovic, "Silicon-photonics networks for global on-chip communication," in *Proc. 3rd ACM/IEEE Int. Symp. Netw.-on-Chip*, 2009, pp. 124–133.
- [6] L. Liu, T. Spuesens, D. Van Thourhout, G. Morthier, L. Grenouillet, N. Olivier, J.-M. Fedeli, P. Rojo-Romeo, P. Rgny, F. Mandorlo, and R. Oroubchouk, "200 mm wafer scale III-V/SOI technology for all-optical network-on-chip and signal processing," presented at the presented at the 7th Int. Conf. Group IV Photon., Beijing, China, Sep. 2010, Conference Paper.
- [7] W. Bogaerts, S. K. Selvaraja, P. Dumon, J. Brouckaert, K. De Vos, D. Van Thourhout, and R. Baets, "Silicon-on-insulator spectral filters fabricated with CMOS technology," *IEEE J. Sel. Topics Quantum Electron.*, vol. 16, no. 1, pp. 33–44, Jan./Feb. 2010.
- [8] L. Liu, G. Roelkens, J. Van Campenhout, J. Brouckaert, D. Van Thourhout, and R. Baets, "III-V/silicon-on-insulator nanophotonic cavities for optical networks-on-chip," *J. Nanosci. Nanotechnol.*, vol. 10, pp. 1461–1472, 2010.
- [9] J. E. Heebner, V. Wong, A. Schweinsberg, R. W. Boyd, and D. J. Jackson, "Optical transmission characteristics of fiber ring resonators," *IEEE J. Quantum Electron.*, vol. 40, no. 6, pp. 726–730, Jun. 2004.
- [10] B. G. Lee, A. Biberman, N. Sherwood-Droz, C. B. Poitras, M. Lipson, and K. Bergman, "High-speed  $2 \times 2$  switch for multiwavelength silicon-photonics networks-on-chip," *J. Lightw. Technol.*, vol. 27, no. 14, pp. 2900–2907, Jul. 2009.
- [11] T. Barwicz, H. Byun, F. Gan, C. W. Holzwarth, M. A. Popovic, P. T. Rakich, M. R. Watts, E. P. Ippen, F. X. Kartner, and H. I. Smith, "Silicon photonics for compact, energy-efficient interconnects," *J. Opt. Netw.*, vol. 6, no. 1, pp. 63–73, Jan. 2007.
- [12] F. Y. Gardes, A. Brimont, P. Sanchis, G. Rasigade, D. Marris-Morini, L. O'Faolain, F. Dong, J. M. Fedeli, P. Dumon, L. Vivien, T. F. Krauss, G. T. Reed, and J. Mart, "High-speed modulation of a compact silicon ring resonator based on a reverse-biased p-n diode," *Opt. Exp.*, vol. 17, no. 24, pp. 21986–21991, Nov. 2009.
- [13] A. Yariv, Y. Xu, R. K. Lee, and A. Scherer, "Coupled-resonator optical waveguide: A proposal and analysis," *Opt. Lett.*, vol. 24, pp. 711–713, 1999.
- [14] J. E. Heebner and Q. Park, "SCISSOR solitons and other propagation effects in microresonator modified waveguides," *J. Opt. Soc. Amer. B*, vol. 19, pp. 722–731, 2002.
- [15] J. E. Heebner, P. Chak, S. Pereira, J. E. Sipe, and R. W. Boyd, "Distributed and localized feedback in microresonator sequences for linear and nonlinear optics," *J. Opt. Soc. Amer. B*, vol. 21, pp. 1818–1832, 2004.

- [16] F. Xia, L. Sekaric, M. O'Boyle, and Y. Vlasov, "Coupled resonator optical waveguides based on silicon-on-insulator photonic wires," *Appl. Phys. Lett.*, vol. 89, p. 041122, 2006.
- [17] J. Capmany, P. Munoz, J. D. Doemenech, and M. A. Muriel, "Apodized coupled resonator waveguides," *Opt. Exp.*, vol. 15, no. 16, pp. 10196–10206, 2007.
- [18] S. Y. Cho and R. Soref, "Apodized SCISSORs for filtering and switching," *Opt. Exp.*, vol. 16, pp. 19078–19090, 2008.
- [19] Y. Vlasov, W. M. J. Green, and F. Xia, "High-throughput silicon nanophotonic wavelength-insensitive switch for on-chip optical networks," *Nature Phot.*, vol. 2, pp. 242–246, Apr. 2008.
- [20] M. A. Popovic<sup>3</sup>, T. Barwicz, M. S. Dahlem, F. Gan, C. W. Holzwarth, P. T. Rakich, H. I. Smith, E. P. Ippen, and F. X. Krtner, "Tunable, fourth-order silicon microring-resonator add-drop filters," *Opt. Exp.*, vol. 17, no. 16, pp. 14063–14068, 2009.
- [21] M. Mancinelli, R. Guider, M. Masi, P. Bettotti, M. R. Vanacharla, J.-M. Fedeli, and L. Pavesi, Optical Characterization of a SCISSOR Device submitted.
- [22] M. L. Cooper, G. Gupta, J. S. Park, M. A. Schneider, I. B. Divliansky, and S. Mookherjea, "Quantitative infrared imaging of silicon-on-insulator microring resonators," *Opt. Lett.*, vol. 35, no. 5, pp. 784–786, Mar. 2010.
- [23] M. Baldi, G. Marchetto, and Y. Ofek, "A scalable solution for engineering streaming traffic in the future internet," *Comput. Netw.*, vol. 51, no. 14, pp. 4092–4111, Oct. 2007.
- [24] M. Masi, R. Orobtcouk, G. F. Fan, and L. Pavesi, "Towards realistic modeling of ultra-compact racetrack resonators," *J. Lightw. Technol.*, vol. 28, no. 22, pp. 3233–3242, Nov. 2010.
- [25] M. Masi and L. Pavesi, Light Combining for Phase Switching preparation.
- [26] K. R. Hiremath, R. Stoffer, and M. Hammer, "Modeling of circular integrated optical microresonators by 2-D frequency domain coupled mode theory," *Opt. Commun.*, vol. 257, no. 2, pp. 277–297, 2005.
- [27] R. Orobtcouk. Villeurbanne, France, Private Communication Université de Lyon.
- [28] R. Orobtcouk, Mode Solver Based on a Full Vectorial Finite Difference Scheme and Developed for Internal Use. Villeurbanne, France, Université de Lyon.
- [29] W. Bogaerts, P. Dumon, D. Van Thourhout, and R. Baets, "Low-loss, low-cross-talk crossings for silicon-on-insulator nanophotonic waveguides," *Opt. Lett.*, vol. 32, pp. 2801–2803, 2007.
- [30] D. D. Smith, H. Chang, K. A. Fuller, A. T. Rosenberger, and R. W. Boyd, "Coupled-resonator-induced transparency," *Phys. Rev. A*, vol. 69, p. 063804, 2004.
- [31] Q. Xu, S. Sandhu, M. L. Povinelli, J. Shakya, S. Fan, and M. Lipson, "Experimental realization of an on-chip all-optical analogue to electromagnetically induced transparency," *Phys. Rev. Lett.*, vol. 96, p. 123901, 2006.
- [32] Y. F. Xiao, X. B. Zou, W. Jiang, Y. L. Chen, and G. C. Guo, "Analog to multiple electromagnetically induced transparency in all-optical drop filter systems," *Phys. Rev. A*, vol. 75, pp. 063833–063836, 2007.
- [33] X. Yang, M. Yu, D. L. Kwong, and C. W. Wong, "All-optical analog to electromagnetically induced transparency in multiple coupled photonic crystals cavities," *Phys. Rev. Lett.*, vol. 102, pp. 173902–173904, 2009.
- [34] D. Lockwood and L. Pavesi, "Silicon photonics II: Components and integration," in *Topics in Applied Physics*. New York: Springer-Verlag, 2011, vol. 119.

**Marco Masi** was born in Milan, Italy, on April 4, 1965. He received the Masters degree in astrophysics from the University of Padua, Padua, Italy. He received the Ph.D. degree from the Nanoscience Laboratory, University of Trento, Trento, Italy, after authoring several articles in astronomy, statistical mechanics, and mathematical physics.

He is currently a Postdoctoral Researcher at the Institut des Nanotechnologies de Lyon Laboratory, Institut National des Sciences Appliquées de Lyon, Villeurbanne, France. His research interests focus on silicon photonics, in particular on the design, modeling, and fabrication of photonic integrated circuits of microresonant structures, its applications to wavelength division multiplexing and interconnect technologies, and possible other areas of physics.

**Mattia Mancinelli** was born in 1985. He received the M.S. degree in physics with a thesis in optoelectronics at the University of Trento, Italy, in 2009, where he is currently working toward the Ph.D. degree in the Nanoscience Laboratory.

His activities are focused in the silicon photonics; he performs both experimental and theoretical characterization of optical integrated circuit for WDM and Telecom applications. He is studying novel coupled micro-resonators configurations to be used for signals processing.

**Alberto Battarelli** was born in Trento, Italy, on December 18, 1968. After working for several years in IT and TLC fields, he received the Masters degree in physics from the University of Trento, Trento, Italy, where he study and verify the behavior of silicon photonic devices based on the SCISSOR concept.

He is currently at Trentino Network, Trento, Italy, a public company that is building an 800 km optical network telecommunication infrastructure for Provincia Autonoma di Trento and other operators expanding it to new large bandwidth services.

**Romain Guider** received the degree in optoelectronics engineering from the École Nationale Supérieure de Sciences Appliquées et de Technologie, Lannion, France, in 2006, and the Ph.D. degree from the University of Trento, Trento, Italy, in 2009.

His doctoral research focused on the study of new nanosilicon waveguides and nanophotonics structures, more particularly on ring and disk resonators. In January 2011, he joined the Institut für Halbleiter und Festkörperphysik, Linz University, Austria, as a Postdoctoral Fellow. His research interests include design, fabrication, and characterization of Si-based photonic structures for on-chip applications.

**Manga Rao Vanacharla**, photograph and biography not available at the time of publication.

**Paolo Bettotti** was born in Italy, on June 18, 1976. He received the M.S. degree (*summa cum laude*) from the University of Padua, Padua, Italy, in 2001, and the Ph.D. degree from the University of Trento, Trento, Italy, in 2005.

He is currently a member of the Nanoscience Laboratory, Department of Physics, University of Trento, Trento, Italy. He was involved with both silicon-based and hybrid materials for integrated optics and sensing applications. His main expertise spans structural and spectroscopical materials' characterization. Moreover, he has a deep knowledge of modeling of complex photonic structures. He is the author of 30 articles in refereed journals and tens of conference papers. He holds an H-index of 12. His research interest includes nanophotonics.

**Jean-Marc Fedeli** received the electronics engineer diploma from the Institut National Polytechnique de Grenoble, Grenoble, France, in 1978.

Then he conducted researches at the CEA-LETI as project leader, group leader, and program manager. For two years, he acted as advanced program director in Memscap company for the development of RF-MEMS, and returned to CEA-LETI in 2002 as coordinator of silicon photonic projects. He works on CMOS (Si rib and stripe waveguides, Si<sub>3</sub>N<sub>4</sub> and a-Si waveguides), Si modulators, Ge photodetectors, SiO<sub>x</sub> material, InP sources on Si, focusing on integration of a photonic layer at the metallization level. He has been participating on different European projects (PICMOS, PHOLOGIC, MNTE, ePIXnet, WADIMOS, PhotonFAB (ePIXfab) and managing the HELIOS project.

**Lorenzo Pavesi** (M'08–SM'11) was born on November 21, 1961. He received the Ph.D. degree in physics from the Ecole Polytechnique Federale of Lausanne, Lausanne, Switzerland, in 1990.

Since 2002 he is Full Professor at the University of Trento, leads the Nanoscience Laboratory, and is dean of the Ph.D. School in Physics. He founded the research activity in semiconductor optoelectronics at the University of Trento, is the president and founder of the IEEE Italian chapter on Nanotechnology, and is an author or co-author of more than 280 papers, several reviews, editor of more than 10 books, author of 2 books and holds six patents.

Dr. Pavesi holds an H-number of 41 according to the web of science. He is a distinguished speaker of the IEEE Photonics society for 2010-2012.